Title
An Investigation of Particle Identification by Energy Loss in Heterogeneous Silicon Detector Systems

Author
Crockett, Wyatt

Publication Date
2018

UNIVERSITY OF CALIFORNIA
SANTA CRUZ

AN INVESTIGATION OF PARTICLE IDENTIFICATION BY ENERGY LOSS IN HETEROGENEOUS SILICON DETECTOR SYSTEMS

A thesis submitted in partial satisfaction
of the requirements for the degree of

MASTER OF SCIENCE

in

PHYSICS

by

Wyatt Crockett

June 2018

The Thesis of Wyatt Crockett
is approved:

Bruce Schumm, Chair

Robert Johnson

Michael Hance

Tyrus Miller
Vice Provost and Dean of Graduate Studies

Table of Contents

List of Figures

List of Tables

Abstract

An Investigation of Particle Identification by Energy Loss in Heterogeneous Silicon Detector Systems

by

Wyatt Crockett

A method of generating energy loss distributions for particles of unit charge with a specific incident momentum through a thickness of silicon is developed. Monte Carlo methods are used to examine the significance of separation between kaon and pion energy loss distributions of the same incident momentum. Several detector configurations, including two homogeneous detectors each composed of 10 layers of 20 μm and 320 μm silicon, and a heterogeneous detector composed of 5 layers of 20 μm silicon followed by 5 layers of 320 μm silicon are simulated. The heterogeneous detector is inspired by the baseline concept of the innermost tracking system at the SiD. For the heterogeneous configuration, the maximum momentum range for a significance of separation of two ($S = 2$) is found to be 700 MeV/c, while the maximum range for $S = 1$ is found to be 940 MeV/c for the heterogeneous configuration. The effect of electronic noise on the kaon pion separation is briefly explored, and found to be small over most of the range of incident momentum for which there is a significant separation between kaons and pions.

1 Introduction

For many years, the use of silicon diode sensors to measure the trajectories of particles arising from the collision of high-energy particle beams has been on the rise. The innermost tracking systems of both the CMS and ATLAS detectors at the Large Hadron Collider are composed primarily of silicon-based tracking layers. Currently under development within the particle-physics community are two designs (the ILC and CLIC) for electron-positron colliding beam facilities. Two of the three detector concepts under consideration for these machines include particle tracking systems composed entirely of silicon-diode sensors.

The high granularity and high precision achievable with silicon diode detectors is well established, making silicon diode sensors a natural choice when precision momentum measurements and vertexing are needed to address physics goals. Less common, though, is the use of silicon tracking systems in the identification of the type of particle passing through the detector ('particle ID'). While the use of the rate of ionization energy loss in gaseous detectors for particle ID is common, it is likely that at least one of the detectors built for the next-generation electron-positron collider will be composed entirely of solid-state sensors, with no gaseous volume for traditional energy-loss measurements.

The ability to perform particle ID measurements via the rate of energy loss could be very advantageous to the study of high-energy electron positron collisions. The Standard Model (SM) of particle physics makes precise predictions about the quark flavor content of the production and decay processes that will be observed in the collisions, and thus flavor-specific precision studies of the electron-positron collision processes provide an important test of the Standard Model and an avenue to probe for new physics. Bottom quarks, produced directly in the electron-positron collisions or through the decays of W, Z and Higgs bosons or the top quark, decay with a strong preference to

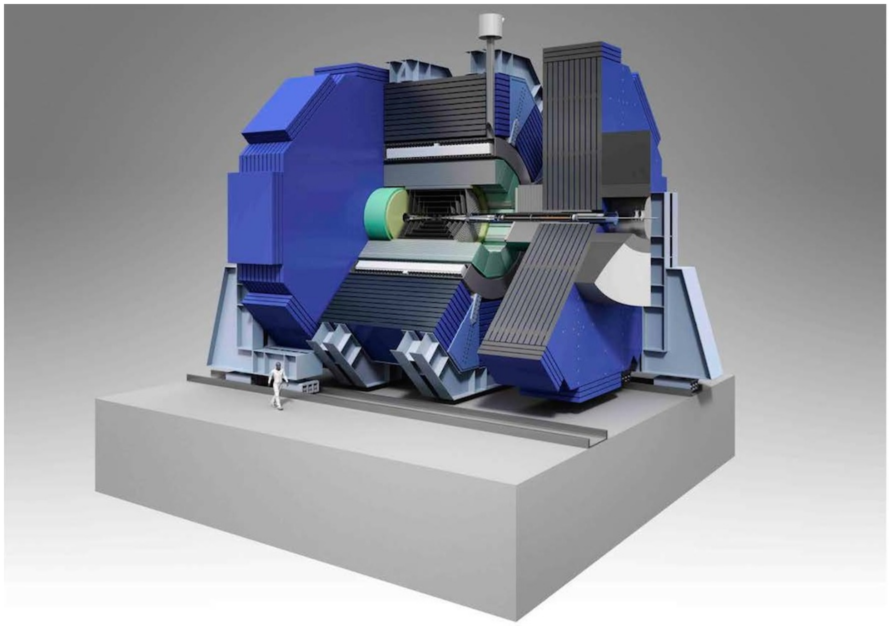

Figure 1.1: A cutaway view of the SiD. SiD stands for Silicon Detector, and it lives up to its name by using an all silicon tracking system.

strange quarks, which in turn produce kaons. Thus, being able to separate kaons from the more commonly-produced pions can be an important tool in SM tests at electron-positron colliders, and in the search for new physics effects.

In addition, several hypotheses about physics beyond the SM, such as Supersymmetry and Universal Extra Dimensions, suggest the possibility that there may be as-of-yet undiscovered massive charged particles with lifetimes great enough to allow them to pass through the detector's tracking system before decaying. If so, a measurement of the rate of energy loss in the tracker would be essential to the demonstration that new particle states were being observed in the collisions.

Of these two motivations for the incorporation of particle ID in electron-positron collider detectors, the first (kaon-pion, or K-π, separation) is the most demanding, so that is what this thesis will focus on.

A rendering of the SiD detector, which is one of the two detectors with an all-silicon tracking system that are currently being designed for future electron-positron linear colliders, is shown in Figure 1.1. The inner five layers are optimized for precision vertexing, and are composed of thin, highly granular, three-dimensional pixel sensors.

The outer five layers are composed of more conventional, and substantially thicker, silicon strip sensors.

The goal of the work presented in this thesis is to develop a Monte Carlo based simulation of the energy loss in silicon diode sensors caused by incident charged particles, and then to use this simulation to explore the particle identification capabilities of such a heterogeneous silicon tracking detector. The significance of separation of pions and kaons as a function of momentum will be the measure used for evaluating the particle identification capabilities of the detector.

1.1 Particle ID via the Rate of Energy Loss

If a particle passes through a detector it will lose some energy. The amount of energy loss depends upon several factors, including the material that the detector is made of, the charge of the incident particle, and the speed of the incident particle. Fortunately, the particle momentum (P) can be determined from the radius of curvature of its trajectory in a magnetic field. The momentum can then be used as a stepping stone towards identifying the particle, and is given by Eq. 1.1:

$$P = \gamma m \beta c \tag{1.1}$$

where, $\beta = v/c$ is the particle speed scaled to the speed of light, γ is the relativistic time dilation factor described in Table 2.1, c is the speed of light, and m is the mass of the incident particle. Since the momentum is independently measured to be known, then the particle mass can be determined from Eq. 1.1 if the speed can be measured. Since each particle has a unique mass, the particle species can be determined immediately.

If two particles have identical momentum but different masses, such as a kaon and pion, then they must have unique velocities. What happens then, if the energy loss distributions of the two particles are inspected? They would have different velocities, and as such would lose energy at different rates while traveling through the detector, causing different energy loss distributions. If the two energy loss distributions can be separated from each other, then the particles may be identified. This is the basis of how these studies will attempt particle identification via energy loss.

Several tracker configurations will be considered: the first two will be homogeneous trackers composed of 10 layers of either 20 μm or 320 μm silicon, the third will be a heterogeneous tracker composed of 5 layers of 20 μm thickness followed by 5 layers of 320 μm thickness. The heterogeneous configuration is similar to the baseline concepts of the SiD and CLIC detectors, where a thin pixel vertexing tracker lies closest to the beam line and a thicker strip tracker lies outside that. However, the need for ultra-precise tracking to exploit the intrinsic reach of electron-positron colliders creates strong pressure to make the innermost sensor layers as thin as possible.

The very aggressive choice of 20 μm for the inner pixel layers is made. While actual sensors are likely to be somewhat thicker than this (the current baseline makes use of 50 μm thick sensors), ongoing pixel R&D might develop workable sensors with a thickness approaching 20 μm. In addition, the use of this aggressive number provides a better sense of the principles and limitations associated with combining information from sensors of very different thickness, and places the most stringent requirements on the development of the simulation code.

1.2 Outline

This thesis will first introduce the mechanisms of energy loss in silicon, as well as the statistics that govern that loss. Then detail will be provided on how to numerically replicate the expected energy loss distributions for use in Monte Carlo simulations. The energy loss distribution generator will be compared to existing experimental and theoretical constraints and modified to reproduce this established behavior. Next, a baseline of separation between a pion and kaon will be established by examining homogeneous detectors, and the effects of electronic noise will be considered. Finally a heterogeneous detector will be examined and an approach to making optimal use of the information from the two separate sections of the detector will be introduced. the resulting performance of the heterogeneous detector will then be compared to that of the two homogeneous detectors.

2 The Energy Loss Model and its Simulation

symbol	definition	value	units
c	speed of light	299,792,458	m/s
β	ratio of speed to c		
γ	$(1-\beta^2)^{-1/2}$		
N_A	Avogadro's number	$6.022 \cdot 10^{23}$	mol^{-1}
N_e	electron density	$3 \cdot 10^{23}$ (Si)	electrons/g
r_e	electron radius	$2.817 \cdot 10^{-15}$	m
m_e	electron mass	510.999	keV/c^2
K	$4\pi N_A r_e^2 m_e c^2$	307.075	keV cm^2/mol
z	charge number		
Z	atomic number	14 (Si)	
A	atomic mass of target	28.0855 (Si)	g/mol
I	mean excitation energy	0.173 (Si)	keV
M	incident particle mass		keV/c^2

Table 2.1: Summary of notation.

2.1 Energy Loss Mechanism in Silicon

It may seem natural that when two identical particles pass through the same absorber, with identical incident momentum, they will not necessarily lose the same amount of energy. This is because energy losses occur due to random interactions between the incident particle and the atoms of the absorber. In the momentum range relevant to the reconstruction of particles from colliding beam experiments, $0.1 \lesssim \beta\gamma \lesssim 1000$, energy losses are dominated by electromagnetic interactions with the absorber's electrons [6]. The random nature of energy loss comes from both the quantity of interactions as well as the amount of energy lost during each interaction. The quantity of energy lost varies partly because there are two types of electromagnetic energy loss: excitation and ionization.

Excitation occurs when an electron that is bound to an absorber atom is excited to a higher energy level, but remains bound to that atom. Due to the quantum nature of bound states, excitations take a well defined amount of energy from the incident particle, as the excited electrons must move between energy levels. There is some variation, however, because an electron can jump multiple levels; this is overcome in Bethe theory by describing a material by a single number, the mean excitation energy, I. This value describes how readily a material takes energy from an incident particle and turns that absorbed energy into electronic excitations [7].

Ionization occurs when the energy that is transferred from the incident particle to an absorber's electron knocks that electron free of the atom it was originally bound to. As the electron is no longer bound to an atom, the energy transfer is not confined to well defined quantities as an excitation would be. The fact that the electron is knocked free allows the possibility of receiving a large amount of energy all at once. The total loss due to ionizations as a particle passes through a thickness of absorber is well described by the Landau distribution, and will be further discussed in the following section.

Finally, the quantity of non-ionizing electromagnetic interactions can be modeled according to the Poisson distribution and will be discussed in more detail in the following section.

2.2 The Landau and Poisson Distributions

The variation of the energy loss of a particle traveling through a medium is described by a combination of the Landau and Poisson distributions. The Landau distribution describes the shape of the total energy lost due to ionizing electromagnetic interactions, while the Poisson distribution describes how many interactions occur as a particle traverses an absorber. The total energy loss distribution that will be generated from these two distributions will be discussed in Section 2.3. The numerical properties of these distributions will be discussed immediately below.

The original Landau probability density function (henceforth, PDF) was described by Lev Landau in 1944 specifically to model the energy loss of fast moving charged particles [4]. The original form of the Landau PDF was written as a complex

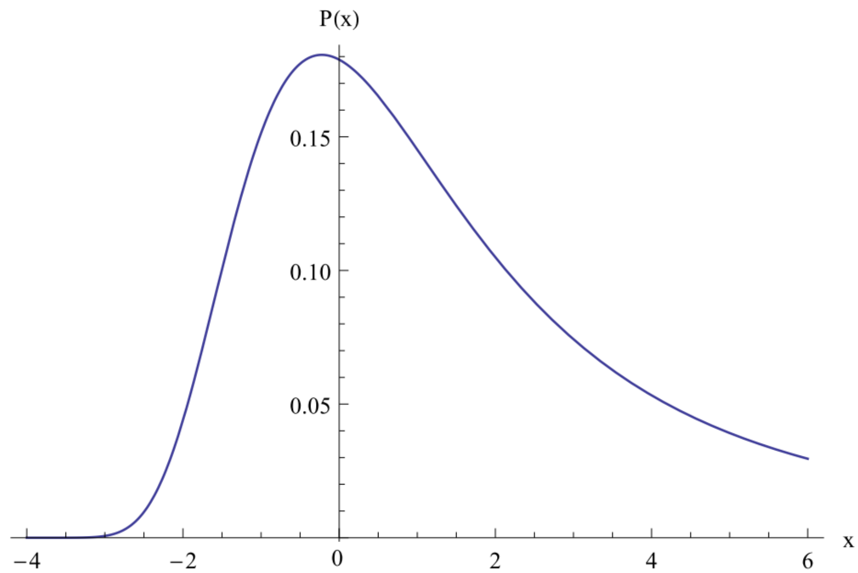

Figure 2.1: The Landau PDF, highlighting the non-vanishing tail.

integral, while the equivalent real integral form is written as Eq. 2.1, which will be used in modeling energy losses due to ionization:

$$p(x) = \frac{1}{\pi} \int_0^\infty e^{-t \ln(t) - xt} \sin(\pi t) dt \tag{2.1}$$

This distribution somewhat resembles a Poisson distribution in shape, but differs in that it is continuous and exhibits a long and thick tail. This tail shape means that the probability of an arbitrarily large x is non-zero, while the negative tail vanishes exactly at $x = -3.809$. In other words, the positive tail is non-vanishing, as is shown in Fig. 2.1. The thick tail can cause significant grief when trying to work with numbers that are Landau distributed. Since the probability of an arbitrarily large x decreases slowly, rather than exponentially, both the mean and variance are undefined for the continuous PDF shown above (Eq. 2.1). When looking at a finite quantity of Landau distributed numbers, a mean and variance can be calculated through normal methods, but they exhibit some odd behaviors. Notably, both the mean and variance tend to increase as the number of trials increases. This leads to the mode (or most probable value) being a much more useful metric than the mean when working with Landau distributed numbers.

The Landau distribution is stable, meaning that if two independent Landau distributed numbers are added together, the result is also Landau distributed. This is

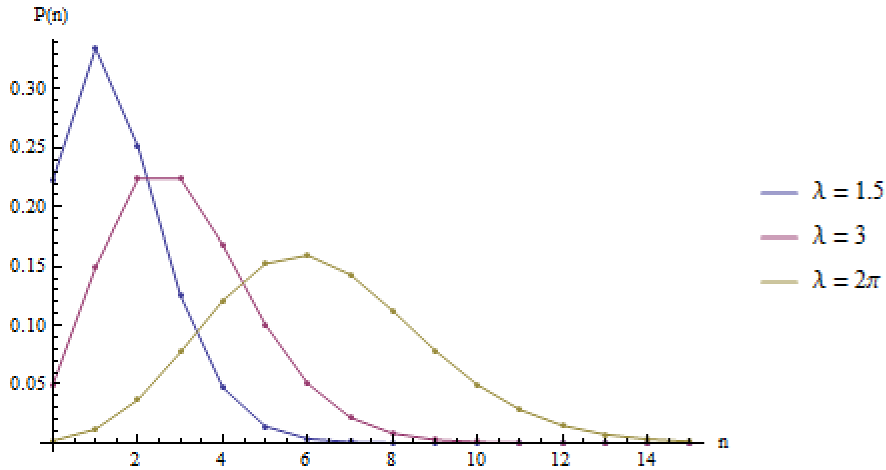

Figure 2.2: Several samples of Poisson probability mass function. All of these λ are possible mean quantities of interactions depending on incident particle energy and silicon layer thickness.

essential for simulating energy loss, as it means that the sum of many Landau distributed losses is also Landau distributed. This distribution also has the property that translating the distribution from side to side is equivalent to taking a Landau distributed number and adding the translation directly to it. These properties mean that the width of a Landau distribution can be changed by simply multiplying a Landau distributed number by some quantity and that the most probable value (or mode, represented by the peak in Fig. 2.1) can be translated by simply adding to a Landau distributed number. The mode and width of Eq. 2.1 are -0.222784 and 4.019 respectively, both of which were found via numerical methods.

The Poisson distribution (Eq. 2.2) describes the probability of n events occurring during an observation where a mean quantity of events, λ, is expected to occur. Since an event either happens or does not happen, the Poisson distribution must be discrete, meaning that n can only be a non-negative integer. The quantity of interactions occurring between an incident particle and the absorber's electrons is Poisson distributed. A handful of Poisson probability mass functions are plotted in Fig. 2.2 to display the general shape of the distribution with various λ.

$$P(n;\lambda) = e^{\lambda}\frac{\lambda^n}{n!} \tag{2.2}$$

While the Poisson distribution has a well defined mean (in fact, the distribution is completely defined by the mean), it is worthwhile to know the mode of the Poisson distribution, as the mode is a much more useful tool than the mean when working with the Landau distribution, and both distributions will be needed. The mode of the Poisson distribution when λ is not an integer is simply the largest integer that is less than λ. The mode then is just the mean, rounded down to the nearest integer. When the mean is an integer the distribution has two modes, λ and $\lambda - 1$.

2.3 The Energy Loss Generator: SimSIdE

The studies in Ch. 3 and 4 will compare the separation of the mean energy losses for pions and kaons to the resolution of those means. To accomplish this, the energy loss of a particle traveling through silicon must be simulated. This will be done by making use of SimSIdE, a routine originally written by Gerry Lynch [5], to simulate the energy loss of an incident particle with some β and unit charge through a thickness of silicon. For this study, SimSIdE was significantly modified (as described below); for instructions on obtaining the modified SimSIdE code, see Appendix A.

SimSIdE simulates the energy loss in two parts: excitation and ionization. SimSIdE does not include any other sources of energy loss, and by extension our simulations will not include any other sources of energy loss. These two parts have been constrained to produce the energy loss behavior that has been extensively studied and parameterized in Ref. [1].

First the energy loss via excitation is found. The excitations are calculated individually for electrons within the K, L, and M shells. For each shell, the mean number of interactions is computed, and from that, a Poisson distributed number of interactions is generated. The mean quantity of interactions is known to be $N_e \delta x (d\sigma/dW) dW$ for an energy loss interval of W to $W + dW$ across a thickness δx[6]. Here, $d\sigma/dW$ is the energy differential cross section for excitation described in Ref. [6]. Since the entire Poisson distribution is defined by the mean (Eq. 2.2), this mean is the only thing that is needed to generate the Poisson distributed number of interactions. Every individual excitation is then simulated based on the shell energy. The excitations within each shell are weighted by a factor of $\frac{1}{E^{\alpha}}$, where E is the maximum energy loss due to excitation (beyond which ionization occurs), and the exponent α has been tuned such that the excitation simulations are within 2% of the predictions of Ref. [1]. Finally, all of the excitations are summed to create the total energy lost to excitation for the passing particle.

The process for simulating the energy lost to excitations is understandably computing intensive. Because of this, SimSIdE includes an option to calculate excitations in lower detail. In the maximum detail case (described above) every single excitation is simulated based on the shell energy. The lower detail settings instead simulate an average excitation energy for each shell and use that average for each excitation within that shell. While the highest detail (level = 3) setting simulated every excitation, the lowest detail (level = 0) setting applies the averaging approach to all excitations. As the detail increases to level = 1, the K shell is simulated fully while the L and M shells use the averaging approach. For a detail level of 2, the K and L shells are fully simulated, while the M shell uses the average value. In the following studies, a detail level of 2 is used, as it offers a significant reduction in run time compared to level 3 while having only a minor ($< 1\%$) impact on precision.

The energy loss via ionizations is calculated by assuming that the total sum of the ionizations across the entire thickness follows a Landau distribution. This is reasonable because the Landau PDF is stable, as discussed in Section 2.2. A number is pulled from a Landau distributed random number generator and is translated and stretched to represent the behavior described in Ref. [1]. This will be discussed in greater depth in Section 2.6. The random number generator used by SimSIdE is the RandLandau function included in the CLHEP library provided by CERN [3]. The documentation for this generator does not state whether it exactly replicates the PDF described by Eq. 2.1, or if it produces some other Landau distribution. To verify that RandLandau replicates Eq. 2.1, the mode and width were examined. The mode was found to be -0.223 (found via numerical methods described in Section 2.6). The full width at half maximum was found to be 4.0 (found by inspecting a histogram of the distribution). These values of the mode and width agree with those described in Section 2.2.

As the mean energy loss (Eq. 2.3) and most probable loss (Eq. 2.6) are well understood [1, 6], one might simply take the known values for the mean energy loss and the width to estimate the separation between incident particle species. However, due to the Landau tail, the separation will not be statistically significant unless the largest energy losses are removed in a process called truncation (discussed in great

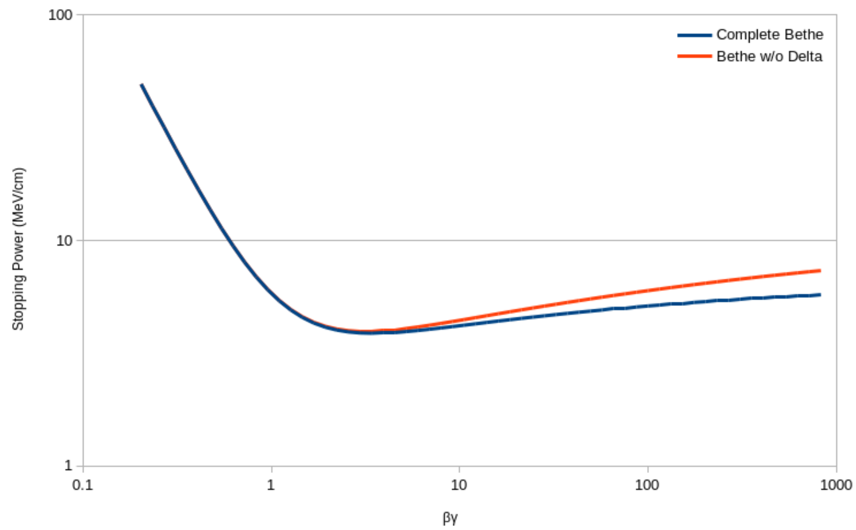

Figure 2.3: A sample comparison of the Bethe curve with and without the density correction. This highlights the effective truncation described by Ref.[6].

detail in Section 3.3). This process changes the energy loss distribution in a fundamental manner, and that change cannot be inferred from Eqs. 2.3 and 2.6. As such, it becomes imperative that the mean and mode of energy loss are understood and that SimSIdE replicates these as closely as possible so that truncation can be utilized to find the best separation possible between the pion and kaon.

2.4 Mean Energy Loss in Silicon

It is clear that simulations must be as realistic as possible, specifically, the energy loss distribution produced by SimSIdE needs to have an appropriate width and positioning. There are two obvious measures of the typical amount of energy lost by a traversing particle: the mean and the mode. The well known Bethe equation (Eq. 2.3) describes the mean stopping power of an absorber primarily due to excitation and ionization of the absorber's electrons:

$$-\left\langle \frac{dE}{dx} \right\rangle = Kz^2 \frac{Z}{A} \frac{1}{\beta^2} \left[\frac{1}{2} \ln \frac{2m_e c^2 \beta^2 \gamma^2 W_{max}}{I^2} - \beta^2 - \frac{\delta(\beta\gamma)}{2} \right] \tag{2.3}$$

where all of the symbols except $W_{\max}$ and $\delta(\beta\gamma)$ are defined in Table 2.1. A sample Bethe curve is shown in Fig. 2.3 for a kaon passing through silicon. The value of $W_{\max}$

can be computed via Eq. 2.4:

$$W_{\max} = \frac{2m_e c^2 \beta^2 \gamma^2}{1 + 2\gamma m_e/M + (m_e/M)^2} \tag{2.4}$$

where all symbols are again defined in Table 2.1. Note that the energy limit $W_{\max}$ depends on the mass of the incident particle. While this means that the Bethe curve has a weak dependence on particle species, in practice the mean energy energy loss depends only on $\beta\gamma$, especially after the truncation procedure described later.

Finally, the symbol $\delta(\beta\gamma)$ is a density effect correction that arises, according to Ref. [6], "As the particle energy increases, its electric field flattens and extends, so that the distant-collision contribution to Eq.(2.3) increases as $\ln(\beta\gamma)$. However, real media become polarized, limiting the field extension and effectively truncating this part of the logarithmic rise." Note that since the density effect correction mitigates the growth of Eq. 2.3, it also will lessen the ability to distinguish between the pion and kaon. Thus it is important to include an accurate model for $\delta(\beta\gamma)$. These studies will use the Sternheimer parameterization of $\delta(\beta\gamma)$, described by Eq. 2.5 [8]:

$$\delta(\beta\gamma) = \begin{cases} x \ln 100 - \bar{C} & \text{if } x \geq x_1; \\ x \ln 100 - \bar{C} + a(x_1 - x)^k & \text{if } x_0 \leq x < x_1; \\ 0 & \text{if } x < x_0 \text{ for insulators/gases.} \\ \delta_0 10^{2(x - x_0)} & \text{if } x < x_0 \text{ otherwise.} \end{cases} \tag{2.5}$$

where all symbols except for x are unitless fitted parameters for a specific absorber material. The x used in Eq. 2.5 is defined as $\log_{10}(\beta\gamma)$. The values of those parameters are listed for silicon in Table 2.2.

parameter	value
a	0.1492
x_0	0.2014
x_1	2.8715
k	3.2546
$\bar{C}$	4.4351
δ_0	0.1400

Table 2.2: Summary of density effect parameters for silicon, listed to the same precision as Ref. [8].

Due to the kinematics of a two particle collision, only so much energy can be transferred between an incident particle and an individual electron during a single event.

This energy limit is represented by $W_{\max}$ within the Bethe equation and is defined by Eq. 2.4 [6]. By limiting the maximum energy transfer, the long and thick tail of the Landau distribution is truncated to be a thick tail with an abrupt end at $W_{\max}$. With this energy limit in place, the mean and variance are no longer undefined and can be studied, despite the variance still being much larger than the mean.

The mean of a distribution is an extremely familiar and efficient metric to compute, making it a natural choice as a measure for comparing the distribution to expectations. Unfortunately, the variance of the energy loss distribution is still prohibitively large, despite the energy cutoff of $W_{\max}$, which grows as $(\beta\gamma)^2$, and thus excludes only the most extreme energy losses (as seen in Fig. 2.1). Without an unreasonable computing time the mean isn't appropriate for comparing SimSIdE to the expected mean from the Bethe equation. Thus, the most probable loss, or mode, of the energy loss distribution will be used instead.

2.5 Landau-Vavilov Most Probable Energy Loss

Since the mean energy loss is not an appropriate method of comparing SimSIdE to real-world expectations, the next obvious choice is the mode of the energy loss distribution. The mode is not sensitive to the high energy Landau tail, representing instead only the most common value, where the PDF is maximal. Graphically this is represented by a peak in the PDF (as seen in Figs. 2.1 and 2.2). Because the mode is not influenced by the size of the largest energy losses, it lacks the weakness that the mean has of being influenced by the Landau tail. In addition, the truncation procedure described later will eliminate contributions from the high energy end of the Landau tail, providing another motivation for constraining the mode rather than the mean of the energy loss distribution.

The Landau-Vavilov most probable energy loss (Δ_p) is modeled by Eq. 2.6 [6]:

$$\Delta_p = \xi \left[\ln \frac{2m_e c^2 \beta^2 \gamma^2}{I} + \ln \frac{\xi}{I} - \beta^2 - \delta(\beta\gamma) \right] \tag{2.6}$$

where all symbols except ξ are described in Table 2.1. The symbol ξ here represents $(K/2)\langle Z/A \rangle (X/\beta^2)$ keV, where X is the thickness of the absorber in cm, and all other symbols are found in Table 2.1. The mode of simulated energy losses from SimSIdE will be compared to this equation in the following section to ensure that the simulations are

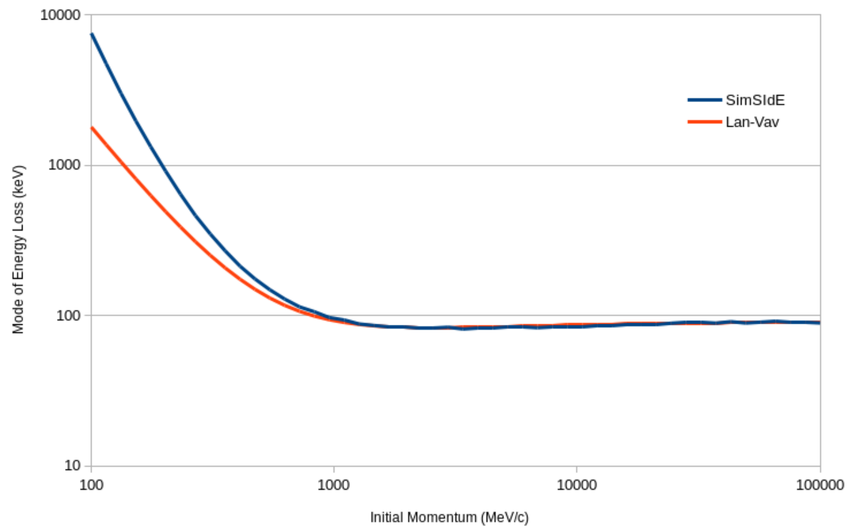

Figure 2.4: Landau-Vavilov most probable loss and SimSIdE mode for a kaon traversing a 320 μm silicon slab. The momentum range of 100 MeV/c to 100 GeV/c is equivalent to $0.2 < \beta\gamma < 203$ for the kaon. Note that the mode of SimSIdE is approximately 5x larger than the Landau-Vavilov most probable value at the lowest momentum.

as realistic as possible.

Figure 2.4 shows an example of the most probable energy loss as a function of momentum, alongside the SimSIdE mode. Note that the mode plateaus at large momenta. This is because the growth in $\langle \frac{dE}{dx} \rangle$ is primarily driven by the growth in the Landau tail, which the mode is not sensitive to. Figure 2.4 also highlights the fact that SimSIdE was originally written to exclusively be used at large momenta. The SimSIdE mode is much too large at low momenta. In Fig. 2.4, the SimSIdE mode is approximately 5x larger than the Landau-Vavilov most probable loss at the lowest displayed momentum. This will be addressed immediately below.

2.6 Scaling SimSIdE

SimSIdE isn't perfect, most notably because it was tuned to agree with expectations at $\beta \simeq 1$. It is necessary to compare the mode of SimSIdE to the Landau-Vavilov most probable loss at a variety of β for the thicknesses and particles involved in these studies. There are four cases to examine, both kaons and pions in 20 and 320 micron thickness silicon. The initial momentum ranges from 100 MeV/c to 100 GeV/c. This range is equivalent to $0.2 < \beta\gamma < 203$ for a kaon and $0.7 < \beta\gamma < 717$ for a pion, so this range lies firmly within the region where ionization and excitation dominate energy losses[6], ensuring that comparing to the Landau-Vavilov most probable loss is appropriate.

The mode produced by SimSIdE must be found for each of these cases at every momentum that is to be compared to the Landau-Vavilov most probable loss. For each point a list is populated by many losses (2^{20} iterations/momentum). The list is then sorted from smallest to largest loss. The algorithm used to find the mode of the ordered list is as follows:

1. An integer N is picked to be the quantity of losses within each interval. In this method, N is picked to be one half of the quantity of entries in the total list.

2. A single interval beginning at an index i and ending at index i+N, is calculated by subtracting the value located at index i from the value located at index i+N.

3. The density of that interval is calculated by taking it and dividing by N, the number of included entries. This means that the more similar the values located at indices i and i+N, the more dense that interval is.

4. The density is found for every valid index. Since N is one half of the quantity of entries, i must run from 0 to N-1.

5. Once the most dense interval of N losses is found, that set of entries is treated as a new list. The algorithm is then repeated from step 1. many times, until only two entries remain.

The mode is taken to be the average of those two final entries. In other words, the mode is found by locating the most dense half, then quarter, then eighth, and so on until only a pair of losses are left. This method is called the "Half Sample Mode" and is a robust estimator of the mode for a sample [2] , provided there is only one peak in the PDF. Using this method to estimate the mode avoids potential issues involving bin width when compared to a histogram approach.

With a method for estimating the mode of SimSIdE, that mode may be inspected and compared to the Landau-Vavilov most probable loss. An example of this was shown in Fig. 2.4, showing that the mode of the original iteration of SimSIdE disagrees with the expected most probable loss at lower momenta. This means that SimSIdE should be scaled to match real world expectations. Two methods of making the SimSIdE mode agree with the most probable loss are considered. The mode of the SimSIdE distribution could be translated to the correct location, or it could be multiplied by a scale factor. These two methods have differing effects regarding the width of the energy loss distribution. A translation would simply move the mode of SimSIdE to the expected value, without changing the width, while a multiplicative scale would change both the position and the width in the same manner, at the same time.

The question becomes: is the width produced by SimSIdE correct? If so, then a translation can be used. If the width of the SimSIdE distribution is too large and on the same scale as the mode being too large, then a multiplicative factor may be sufficient. The intrinsic width of the Landau PDF is 4.019 (Section 2.2). According to Ref. [1], the normalized Landau width of 4ξ then is appropriate for large thicknesses ($\sim$ 1cm) of silicon. However, Ref. [1] also demonstrates that thinner layers require an expansion of the Landau width. For a particle with $\beta\gamma \gtrsim 100$, the width in 20 μm Si is expanded by a factor of 2.465, and the width in 320 μm Si is expanded by 1.382. Compiled in Table 2.3 is a comparison of the expected widths to the width of SimSIdE.

Species	Thick(μm)	$\beta\gamma$	Mom.(GeV/c)	4ξ(keV)	Exp.(keV)	SS(keV)*
pion	20	100.31	14.00	1.43	3.34	3.20
pion	320	100.31	14.00	22.81	31.57	31.00
kaon	20	100.17	49.45	1.43	3.34	3.20
kaon	320	100.17	49.45	22.81	31.57	32.00

Table 2.3: Summary of thickness dependent widths where Exp. and SS are abbreviations for Expected and SimSIdE respectively. Expected widths are from Table VI in Ref. [1]. *Estimated from a histogram of the SimSIdE energy distribution.

Table 2.3 makes it clear that the widths produced by SimSIdE are appropriate, thus a translation rather than a multiplicative scale is sufficient to make the mode of SimSIdE agree with the most probable loss.

However, upon further inspection of the original SimSIdE code, it was noticed that a high energy approximation is used when establishing the mode of the ionization Landau curve. The can be shown by histogramming the individual excitation and ionization energy distributions produced by SimSIdE as shown in Fig. 2.5. This is corrected by replacing the value of the ionization energy loss mode with a more computing

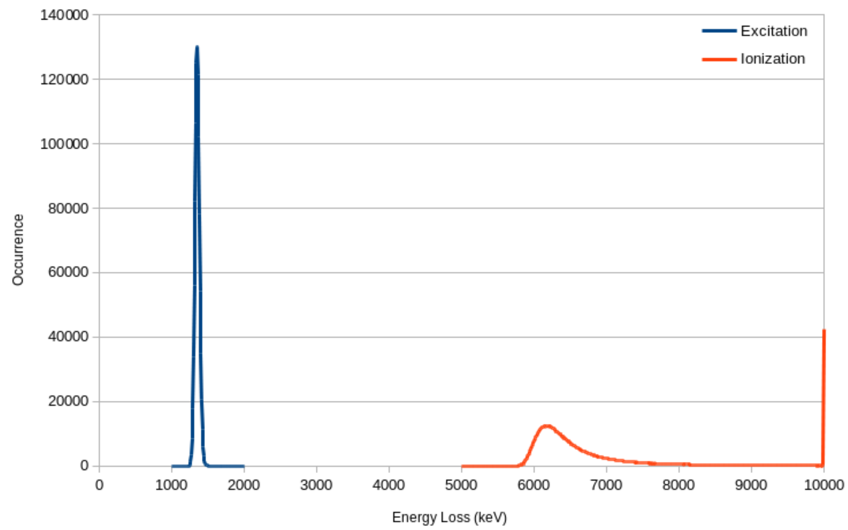

Figure 2.5: Separated excitation and ionization distributions for a 100 MeV/c kaon in 320 micron silicon. The positioning of the ionization distribution is far too far to the right, causing the discrepancy shown in Fig. 2.4. The spike in the ionization distribution is due to the last bin being an overflow bin, encompassing all losses greater than 10 MeV.

intensive, but more accurate, value. This value is provided by the most probable loss as described in Eq. 2.6 after subtracting away the mode of the excitation energy loss distribution. The mode of the excitation energy loss distribution is determined by the mode of the Poisson-distributed quantity of interactions and the mean energy loss from each shell.

This correction places the SimSIdE mode close to the values calculated from Eq. 2.6. Figure 2.6 shows all of the corrected SimSIdE modes along their Landau-Vavilov counterparts. Figure 2.7 shows that the ratios of the Landau-Vavilov most probable loss to the SimSIdE mode in all four cases (pion/kaon and 20/320 μm) are close to 1. Finally the slight negative trend of those ratios can be fit by the function $F = 0.977530 - 0.017845 \ln(\beta\gamma)$ to provide the final a small scaling correction.

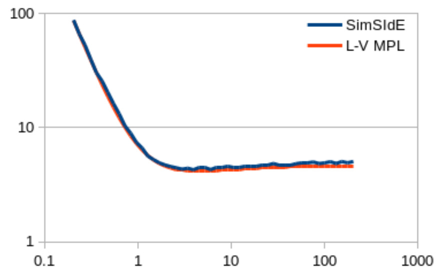

(a) Kaon in 20 micron silicon

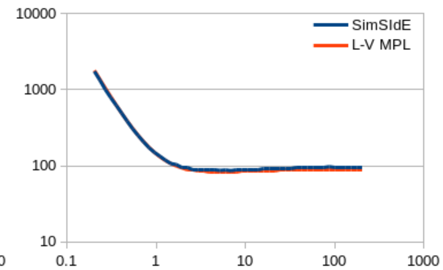

(b) Kaon in 320 micron silicon

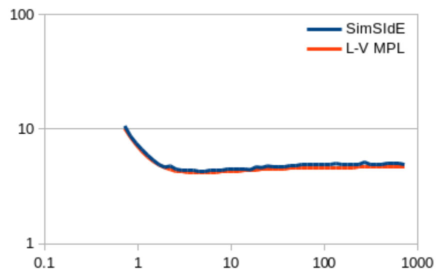

(c) Pion in 20 micron silicon

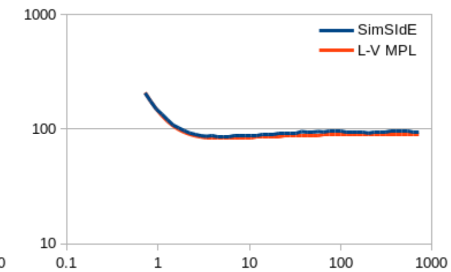

(d) Pion in 320 micron silicon

Figure 2.6: Adjusted SimSIdE modes and the Landau-Vavilov most probable losses in keV as functions of $\beta\gamma$. These $\beta\gamma$ ranges are identical to 100 MeV/c to 100 GeV/c.

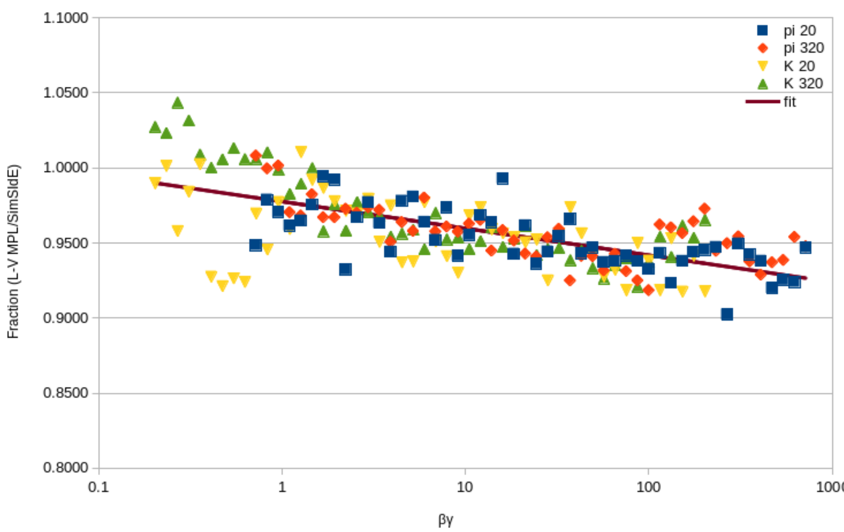

Figure 2.7: Ratios of the Landau-Vavilov most probable value to the SimSIdE mode for all cases, across the momentum range 100 MeV/c to 100 GeV/c.

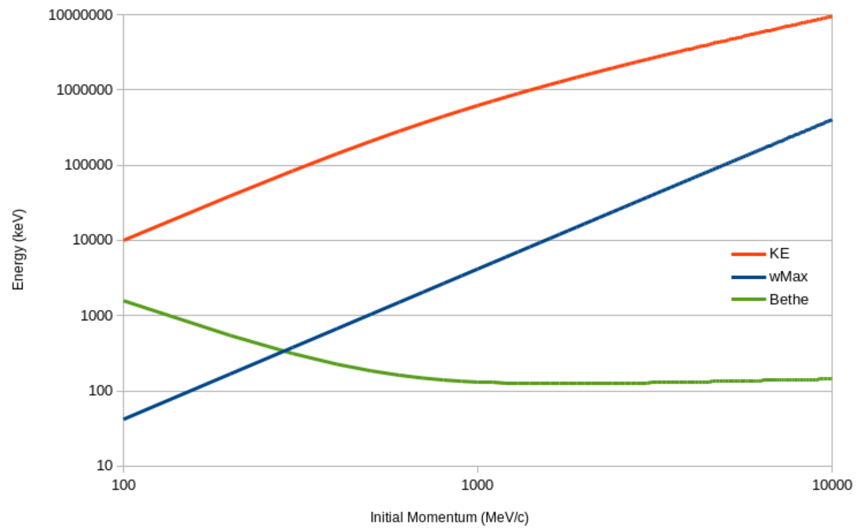

Figure 2.8: A comparison of kinetic energy, W_{max}, and mean energy loss according to the Bethe equation with Sternheimer corrections. These calculations all assume a kaon incident upon 320 micron silicon. The displayed momentum range (100 MeV/c to 10 GeV/c) is equivalent to $0.2 < \beta\gamma < 20$.

2.7 Maximum Energy Loss

Another flaw of SimSIdE is that it does not include an upper limit on the quantity of energy that can be lost by a single incident particle. While this is in perfect accordance with the long and thick tail of the Landau distribution, it is unphysical when $\beta < 1$. There exist two natural limits on the energy loss. In addition to $W_{\rm max}$, the maximum loss from a single collision, it is also obviously true that the particle can't lose more that its incident kinetic energy. Beyond that point the particle would be absorbed completely by the silicon. The other limit, $W_{\rm max}$, is a reasonable upper limit for higher momentum incident particles where a single large energy transfer is expected to dominate the entire energy loss. Figure 2.8 shows that there is a region of momenta where the expected mean energy loss (Bethe) is much greater than $W_{\rm max}$, implying that at lower momenta there must be multiple energy transfers on the order of $W_{\rm max}$.

The solution employed here is to make use of the Poisson distributed number of interactions introduced in Section 2.2 to scale up $W_{\rm max}$ by an appropriate amount. After a slight change to SimSIdE to allow the routine to pass back the number of interactions, the total energy limit across the entire silicon slab can be computed. Since the Poisson distribution includes zero, the exact number that $W_{\max}$ is scaled by is the number of interactions from SimSIdE plus one, since the minimum limit should be $W_{\max}$. Enforcing an upper limit on energy loss significantly reduces the variance of the energy loss.

There is one caveat to this method of computing an energy limit. $W_{\max}$ is the maximum energy transfer per interaction, and as such, it would be most realistic if it were recalculated between each interaction. This is not really possible, however, because any large energy loss will be due to the thick Landau tail, and SimSIdE determines ionization all at once for the entire layer of Silicon. Since there is no differentiating between individual ionizations, there is no way to update $W_{\max}$ between interactions. If it was possible to update $W_{\max}$ between ionizations, it would always decrease, as energy is transferred from the incident particle to the absorber's electron, the incident particle must slow down, decreasing $\beta\gamma$, and thus decreasing $W_{\max}$. The take away of this caveat is that it is expected that the energy limit used here overestimates the real energy transfer limits, especially since any single large energy transfer would severely dampen $W_{\max}$.

The overestimation of maximum energy loss will not matter in the studies, however, due to the layer truncation procedure required to mitigate the statistical effects of the Landau tail. This will be discussed in detail in Section 3.3.

2.8 Mean Case Study

While the mean energy loss across a single slab of absorber is problematic to work with and is too unreliable to be used on its own, it is still interesting to see the average effects of correcting the ionization positioning, applying the slight fractional scale factor, and enforcing energy limits upon losses. Figure 2.9 summarizes these changes to SimSIdE. Note that the variance is large and causes significant jitter, which is reduced after enforcing energy limits. The fact that the SimSIdE mean consistently overestimates the Bethe calculation highlights the effects of the caveat discussed in Section 2.7.

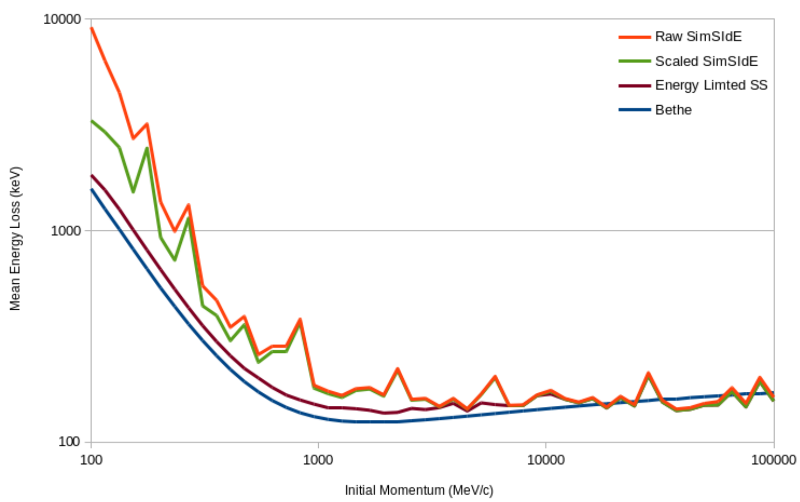

Figure 2.9: Comparison of mean energy loss for a kaon through a 320 micron silicon slab with various rules (scaling, energy limits) applied. The Raw SimSIdE curve shows what would be obtained if SimSIdE was used in its original form, without any interference. The Scaled SimSIdE curve shows the output of SimSIdE after fixing the translation of the ionization curve and applying the slight scale factor determined in Section 2.6. The Energy Limited SimSIdE curve is the final version, after fixing translation, scaling, and then enforcing energy limits. The large fluctuations in the SimSIdE mean illustrate the difficulty of using the mean energy loss to assess and correct the overall scale.

3 Pion-Kaon Particle ID in a Homogeneous Detector

3.1 A Layered Detector

With a method in hand that implements SimSIdE so that it accurately replicates real world expectations across a wide range of β, it is now possible to model how well a multi layer semiconductor tracker can be used to differentiate between pions and kaons. Recall from Section 2.3 that SimSIdE only depends on the speed (β) of the incident particles and the thickness of the silicon layer when it simulates the energy distribution of particles passing through a single thickness of silicon. The energy loss from SimSIdE is then scaled according to Section 2.6 and limited according to Section 2.7. The mass of the particle only plays an extremely small role in this process via the energy limit of W_{max} (Eq. 2.4). This means that a pion and kaon with the same β traveling through the same individual silicon slab will behave nearly identically.

However, the momentum of the incident particles is assumed to be already known from the radius of curvature in the tracking system of the hypothetical detector. If two particles have the same momentum, but different masses, then they will have different speeds, as well as different kinetic energies. Their energy loss distributions can be modeled, and if those distributions are separable, then the particles can be identified.

This particle identification process is greatly improved by including many layers in the detector for two reasons. First, using many layers allows for the layers where the highest energy losses occur, those that inhabit the Landau tail, to be excluded from the total mean energy loss. This process, called "truncation" reduces the mean somewhat, while reducing the variance significantly. In addition, if both particles start with the same momentum, and they each lose (by chance) the same energy, that energy loss will be different fractions of their kinetic energy. In other words, one particle will slow down more while the other will slow down less. This process will affect the total energy loss distributions across many layers.

This will be the basis for separating the two particles: run each through the same layered detector many times with the same incident momentum, find the mean energy loss across several layers, and compare that mean for each of the particles in units of total variance. This allows several potential studies to be done, including separation in homogeneous detectors as well as separation in a heterogeneous detector inspired by the proposed tracking systems of the SiD and CLIC detectors.

In this chapter the tools needed to simulate and optimize the performance of a homogeneous multi-layer tracker, i.e., one for which all layers are the same thickness, are discussed. Then two such homogeneous trackers: one composed of 10 layers of 20 μm silicon and the other of 10 layers of 320 μm silicon, are simulated. These studies will form an important baseline for comparison with the performance of the heterogeneous detector.

In these studies, it will be assumed that the detector readout makes a perfect, stable, noise-free measurement of the energy loss in the sensor. While this is certainly not true in reality, in practice the Landau fluctuations discussed at length in the previous chapter dominate other experimental shortcomings in most situations. Electronic noise will be briefly examined in Section 3.7 to verify that the impact is minor.

3.2 Absorption

The smallest incident particle speeds included in these studies leave certain particles with very little kinetic energy of their own. The slowest case, for example, is a 100 MeV/c kaon; at this momentum the kaon only has 10.0 MeV of kinetic energy. The expected loss (or mean stopping power) for this particle traversing a 320 μm layer can be calculated from Eq. 2.3 to be 1.56 MeV. It is clear then that a 100 MeV/c kaon is unlikely to make it through 10 layers of 320 μm silicon, and a rule for determining when a particle is absorbed must be developed.

For each case (pion/kaon and 20/320 μm) there exists a β at which the particle's kinetic energy is equal to the mean loss calculated from Eq. 2.3. In other words, there is a speed at which the average particle is absorbed in a layer of the detector. The rule used in these studies will be that if a particle falls below this threshold β then the particle will be considered absorbed, with the loss for that layer being set equal to its remaining kinetic energy. In the event that a particle is absorbed, the energy loss for the remaining layers will be set equal to zero, as the particle has stopped moving and has no more energy to give. In the truncation procedure described below, layers for which the particles traverse the sensor are maintained in the energy loss sum, since this provides additional information about the speed of the incoming particle.

3.3 Truncation

Studying the particle identification performance of a multi-layer detector requires a new tool called "truncation," which is useful when trying to maximize the separation between pions and kaons. Here, truncation means omitting certain layers from the summed total loss across a detector. The notation used will be that a truncation of zero ($T = 0$) means that no layers are omitted, a truncation of one ($T = 1$) means that the layer where the largest energy loss occurred will be omitted, a truncation of two ($T = 2$) means the two largest losses are omitted, and so on.

Truncation in this manner has several effects. First, by omitting the largest losses that occur through a detector, the tail of the Landau distribution is effectively removed. Also, the skewness of the energy loss distribution is reduced with increased truncation up until a point, typically as T approaches the total number of layers, where additional truncation begins to increase skewness. Another benefit of truncation is that since it excludes the largest losses, it renders the fact that the energy limits discussed in Section 2.7 are overestimated to be a non-issue. This is because the rare energy loss that falls within the extension on the energy limit will likely be filtered out by a truncation of just $T = 1$, and will almost certainly be filtered out by any higher truncation. Most importantly though, truncation greatly reduces variance, allowing the mean energy loss to be used much more effectively for separating the pion and kaon. Figure 3.1 shows the evolution of the energy loss distribution from a Landau shape towards a Gaussian shape as truncation increases. An example of the numerical effects of truncation are shown in Table 3.1 by examining the mean loss of a kaon with an incident momentum of 10 GeV/c.

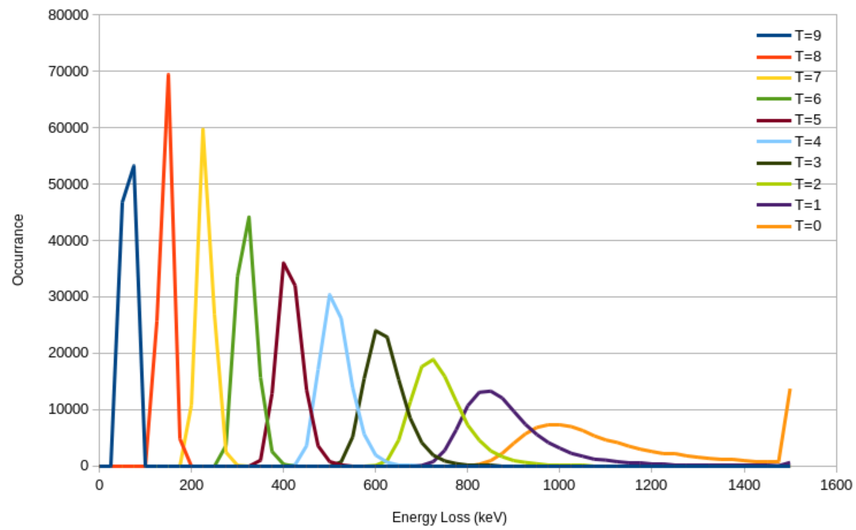

Figure 3.1: Energy loss distributions for a 10 GeV/c kaon passing through 10 layers of 320 micron silicon with various truncations. Note that only the $T = 0$ distribution has a large overflow bin. Extremely large losses, like those that would populate overflow bins, and almost completely removed by a truncation as low as $T = 1$.

T	9	8	7	6	5	4	3	2	1	0
μ	75.6	156.9	242.7	332.8	427.4	527.5	635.2	755.5	908.8	1648.6
σ	5.8	10.4	15.1	20.4	26.5	34.3	45.4	66.5	181.2	14560.6

Table 3.1: Truncation example for a 10 GeV/c kaon traversing a detector of 10 layers of 320 micron silicon. The mean (μ) and variance (σ) are in keV. Note how quickly the variance drops with truncation for small numbers of truncated layers.

3.4 Significance of Separation

The next step is to pick a quantitative measure of how well the pion and kaon can be separated. This measure is the significance of separation (S), defined as Eq. 3.1.

$$S = \frac{|\mu_\pi - \mu_K|}{\sqrt{\sigma_\pi^2 + \sigma_K^2}} \tag{3.1}$$

Where the mean is denoted by μ and the variance is σ. In other words, S is the separation of the pion and kaon means in units of total variance. The larger the significance of separation, the more reliably the pion and kaon can be distinguished from each other.

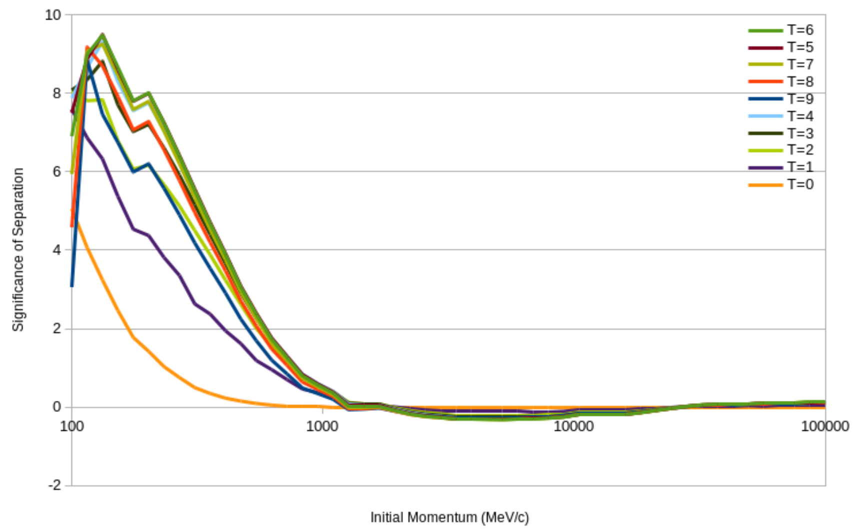

Figure 3.2: Composite significance of separation for all truncations of a homogeneous detector composed of 10 layers of 20 μm silicon. The legend is ordered from highest significance to lowest, matching the graph.

The goal of the homogeneous layer studies is to learn what value of T yields the most significant separation, and to find the momentum range over which pions and kaons can be separated.

3.5 Homogeneous 20 Micron Silicon Detector

Initially, two homogeneous detector layouts will be considered, to serve as a base line to compare the heterogeneous detector to in terms of significance of separation. The first will be a detector constructed from 10 layers of 20 μm silicon. The significance of separation will be found for all truncations across the momentum range 100 MeV/c to 100 GeV/c, as shown in Fig. 3.2.

Although somewhat busy, Fig. 3.2 shows that truncations of $T = 5$ and $T = 6$ are very similar for this detector configuration, and that those truncations provide the highest significance of separation for incident momenta less than 1 GeV/c. It also confirms that the significance of separation is greatly improved by truncation, but too much truncation will inhibit the ability to separate the two distributions. Finally, Fig. 3.2 shows that the significance of separation is small beyond an initial momentum of

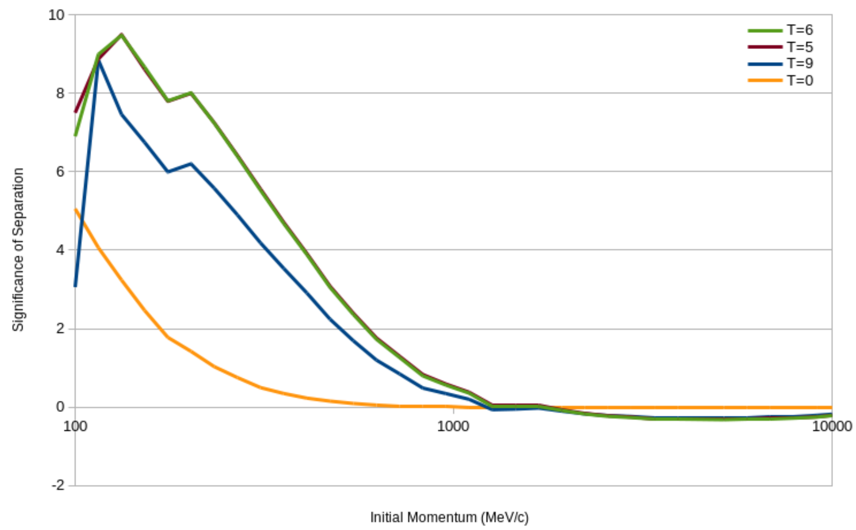

Figure 3.3: Selected significance of separation plots for a homogeneous detector composed of 10 layers of 20 μm silicon. The plots shown here are for the minimum ($T = 0$) and maximum ($T = 9$) truncations, as well as the maximum significance of separation ($T = 5, 6$). For the most part, the $T = 6$ curve lies slightly above the $T = 5$ curve.

∼800 MeV/c. With that in mind, Fig. 3.3 has been created from the same data as Fig. 3.2, but only displays truncations of $T = 0, 5, 6, 9$ in the momentum range of 100 MeV/c to 10 GeV/c, in order to give a more clear picture of what is observed.

The general shape is expected: at the lowest momenta the incident particles don't have much energy to lose. As they gain momentum they have more energy to relinquish, increasing the mean loss and the numerator of Eq. 3.1. However, the faster the particles traverse the detector, the less time they spend inside, transferring less energy, thus decreasing the difference in the means. The maximum significance of separation for the 20 μm detector is observed at ∼130 MeV/c, and is the incident momentum for which the decrease in mean energy loss starts to dominate the increase in the kinetic energies of the incident particles.

Figure 3.4 shows the individual contributions to the significance calculation (Eq. 3.1) for the optimal truncation $T = 6$ curve from Figures 3.2 and 3.3. Shown are the individual means and variances for pions and kaons, as well as the significance of separation. The small rise in significance at approximately 175 MeV/c appears to be due to a flattening of the kaon mean energy loss in that region while the kaon variance

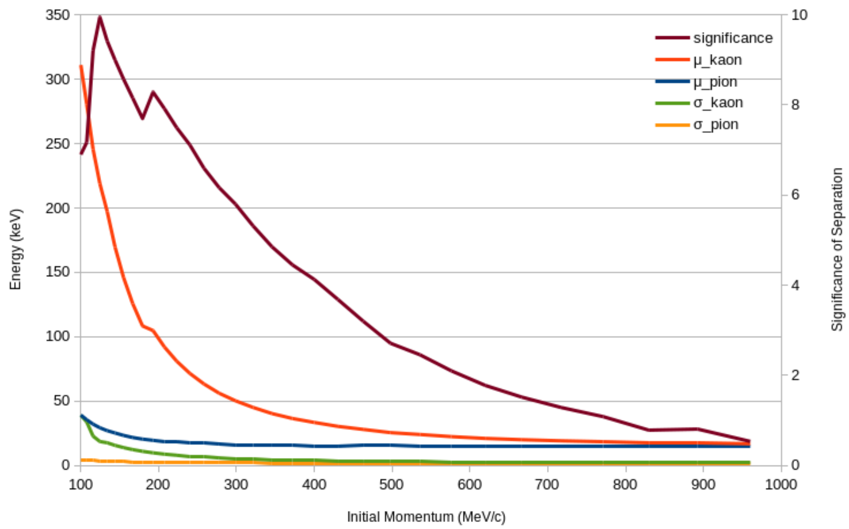

Figure 3.4: Truncated mean losses, variances, and significance for $T = 6$ for a detector composed of 10 layers of 20 μm silicon. The small increase in significance at ∼175 MeV/c is due to the local flattening of the mean loss from kaons in that region.

is still decreasing. Determining the cause of this flattening would require further study.

Overall, is it seen that for the homogeneous 10 layer 20 μm detector that a truncation of 5 or 6 produces the optimal separation over the full range of momentum for which a significant separation can be achieved. The following momenta and significances were all found for a truncation of $T = 6$, as the $T = 5$ curve only exceeds the $T = 6$ curve at the lowest momenta. At an incident momentum of 150 MeV/c (the momentum at which kaons reliably make it through 10 layers of 320 μm silicon), the separation is found to be 8.62. At an incident momentum of 230 MeV/c (the incident momentum that provides the most significant separation in the 320 μm tracker) the separation is 7.21. The significance of separation exceeds $S = 2$ up to 581 MeV/c and exceeds $S = 1$ up to 765 MeV/c.

3.6 Homogeneous 320 micron Silicon Detector

Before a deeper investigation of the ten layer 320 μm tracker can begin, the relevant incident energy range must be determined, since low energy kaons that would pass all the way through a detector composed of 20 μm layers would be absorbed by a detector

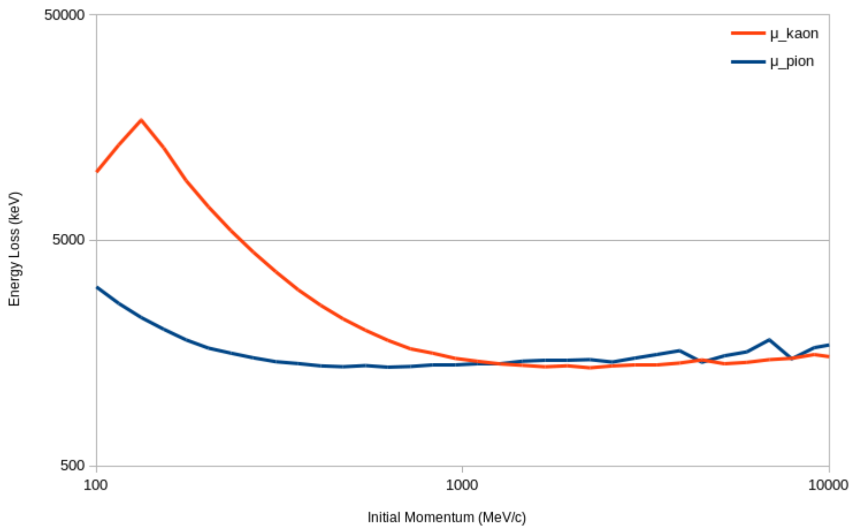

Figure 3.5: Mean losses in a tracker composed of 10 layers of 320 μm thick sensors at a truncation of $T = 0$. Note the sharp peak in the kaon mean energy loss at 150 MeV/c. Up to that momentum kaons are being absorbed inside the detector, while after that point the kaons are passing all the way through. The noise observed at the higher momenta is because this truncation doesn't filter out the Landau tail.

composed of 320 μm sensors. In this case, a pion of the same momentum would penetrate the 320 μm tracker, leaving a signal in the outer detector (hadronic calorimeter) that would clearly distinguish it from the kaon. This is a very reliable way to separate low momenta pions from kaons, and so here there is no need to consider momentum below this threshold.

Figure 3.5 shows the mean energy loss in a 320 μm tracker as a function of incident momentum, separately for pions and kaons. The peak in the mean kaon energy loss at 150 MeV/c indicates that this is the energy for which the kaon begins to penetrate the entire detector and enter the calorimeter. Thus, for the 320 μm tracker as well as the heterogeneous tracker of Ch. 4 our studies will extend down to only 150 MeV/c.

With the lower limit of 150 MeV/c in place, Fig. 3.6 is unsurprising, with the general shape being the same as that of the 20 μm homogeneous detector. The 320 μm tracker displays a higher maximum significance as expected since the ratio of the mean variance to the mean energy loss is smaller for the 320 μm tracker than the 20 μm tracker. Figure 3.6 shows that a truncation of $T = 7$ yields the maximum significance

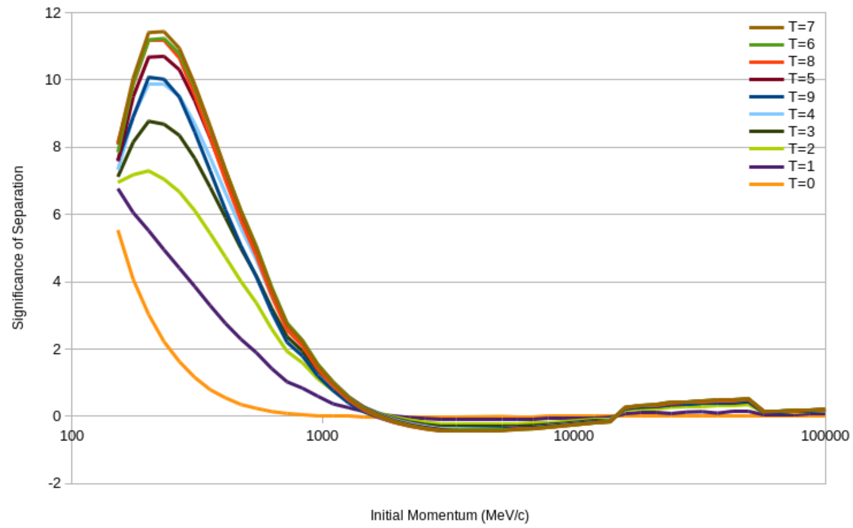

Figure 3.6: Composite significance of separation for all truncations of a homogeneous detector composed of 10 layers of 320 μm silicon for momenta beyond 150 MeV/c.

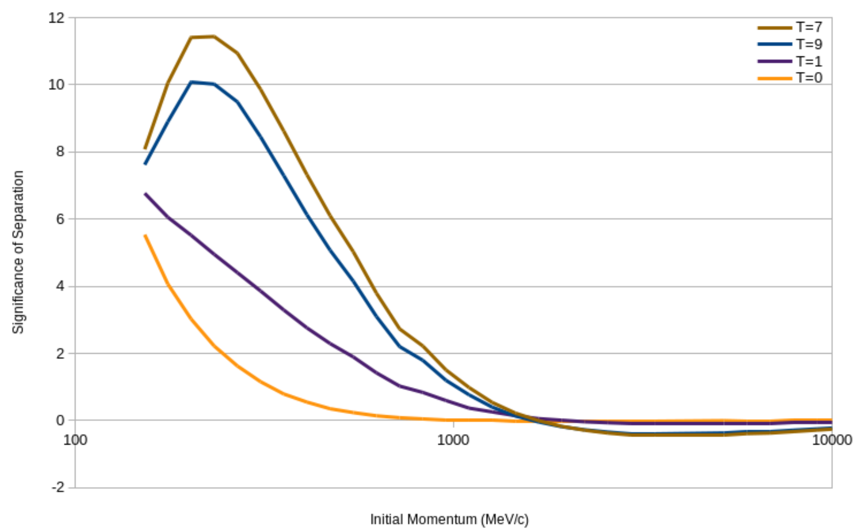

Figure 3.7: Selective significance of separation plots for a homogeneous detector composed of 10 layers of 320 μm silicon for momenta above 150 MeV/c. The plots shown here are for the minimum and maximum truncations, as well as the maximum significance of separation. The $T = 7$ curve yields the greatest significance of separation over the displayed range.

of separation across the displayed momentum range, somewhat higher than the optimal value for the 20 μm tracker, which was $T = 6$. It also confirms that the significance is low beyond an incident momentum of ∼1 GeV/c.

Figure 3.7 shows the significance as a function of incident momentum for selected values of T. The $T = 0, 1$ curves are included to illustrate that a large truncation gives a significant improvement in the separation. $T = 7$ is the optimal truncation value, while the $T = 9$ curve is shown to illustrate that the significance degrades for truncations beyond $T = 7$.

Thus, it is concluded that energy loss particle identification for a 320 μm tracker is only relevant for incident momenta at and above 150 MeV/c. The following momenta and significances were all found using the optimal truncation of $T = 7$. At the minimum incident momentum of 150 MeV/c, the significance of separation is 8.14. At an incident momentum of 230 MeV/c the significance of separation is 11.3. The separation exceeds $S = 2$ up to an incident momentum of 842 MeV/c, and the separation exceeds $S = 1$ up to 1020 MeV/c.

To summarize, Table 3.2 shows four measures of the particle identification performance for the 10 layer homogeneous trackers: the significance of separation at an incident momentum of 150 MeV/c, the maximum significance of separation (at 230 MeV/c for the 320 μm tracker), the maximum incident momentum for which pions and kaons can be separated by $S = 2$, and the maximum incident momentum for which pions and kaons can be separated by $S = 1$. These values will be used as a baseline of comparison for the heterogeneous tracker, which is presented in the next chapter.

tracker	T	S_{150}	S_{230}	$2S$(MeV/c)	$1S$(MeV/c)
20 μm	6	8.62	7.21	581	765
320 μm	7	8.14	11.3	842	1020

Table 3.2: Summary table of four points of comparison in the homogeneous trackers. S_{150} represents the significance at 150 MeV/c, the lowest momentum at which kaons reliably penetrate into the calorimetry. S_{230} is the significance at 230 MeV/c, the momentum at which the highest significance has been observed (as the peak of the 320 μm tracker), $2S$ is the upper momentum limit at which a significance of $S = 2$ is observed. $1S$ is the upper momentum limit at which a significance of $S = 1$ is observed.

3.7 Electronic Noise

Throughout this study, the contributions of electronic noise to the spread of the energy loss distribution has not been considered. In this section, the validity of this assumption is explored by adding in an additional Gaussian contribution to each layer's energy deposition. The Gaussian distribution is centered on zero, since electronic noise is as likely to subtract from the overall collected charge as it is to add to it.

In general, the channels of a multi-channel solid state tracking systems require a median signal-to-noise of 12:1 or greater in order to adequately suppress the noise-induced hit rate while maintaining efficiency for sensing through-going tracks. Thus, the width of the Gaussian is set to be 1/12 of the median charge deposition for a minimum ionizing track that passes through the layer ($\beta\gamma \sim 3$), corresponding to a median energy loss of 5.3 keV for a 20 μm thick layer, and of 98 keV for a 320 μm thick layer.

tracker	T	S_{150}	S_{230}	$2S$(MeV/c)	$1S$(MeV/c)
20 μm	6	8.61(8.62)	7.15(7.21)	570(581)	751(765)
320 μm	7	8.10(8.14)	11.1(11.3)	775(842)	987(1020)

Table 3.3: Summary table of four points of comparison in the homogeneous trackers with added electronic noise. The noise-free simulations have been included in parentheses for ease of comparison.

Table 3.3 shows the comparison between the performance of both the 20 μm and 320 μm homogeneous detectors with and without noise, for the four comparison points at the optimal truncations for the noise-free detector. The 20 μm homogeneous detector suffered less than a 1% difference for peak significances, and less than 2% for the $S = 1$ and $S = 2$ ranges. The 320 μm homogeneous detector suffered less than 2% difference for peak significances, but up to 12% for the $S = 1$ and $S = 2$ ranges. The significant effects of electronic noise, especially on the 320 μm configuration, warrant additional study.

4 | Pion-Kaon Particle ID in a Heterogeneous Detector

The heterogeneous tracker that we'll discuss in this chapter is composed of 5 layers of 20 μm thickness followed by 5 layers of 320 μm thickness. This configuration reflects the base concepts of the SiD and CLIC detectors, where a thin pixel vertex tracker lies closest to the beam line and a thicker strip detector lies outside that.

There is one thing to address before studying this tracker configuration: truncation. For the heterogeneous tracker, truncation will almost always remove the 320 μm layers first, since they are 16 times thicker than the 20 μm layers, and will be very likely to have the largest energy loss. This is undesirable because the energy losses in the thinner layers tend to have higher variance relative to the mean energy loss [6]. This is verified by Sections 3.5 and 3.6, which show that the 320 μm detector yields a higher significance than the 20 μm detector. There are several ways to address this issue, two of which were considered: the truncation could selectively remove thin layers before thick layers, or the thin layers could be weighted by some multiplier, allowing them a higher chance of being truncated.

The second option is chosen because an energy loss in a thin layer that is close to the mean of the distribution in that layer carries more information about the particle's velocity than an energy loss in a thicker layer that's far above its mode. It also provides a second parameter (in addition to the truncation parameter T) over which the particle identification performance can be optimized. Thus, such an approach would be expected to lead to a more efficient use of the information at hand. To be clear, the weighted simulation runs identically to the unweighted heterogeneous tracker simulation: the simulated losses (between particle energy updates, or between layers) are not changed by weighting. The only difference is in the recording of the losses. The weighted layers are recorded with their weight multiplied in, then truncation can take place on the weighted losses. The significance is then computed from those weighted and truncated losses.

The weighting procedure was done for a wide range of thin to thick weights, including 1:1, 4:1, 8:1, and so on up to 40:1. As in Chapter 3, four points of comparison are used in evaluating the particle ID performance. The first two are the observed significance for incident particle momenta of 150 MeV/c (the energy below which kaons tend to get absorbed and don't exit the tracker) and 230 MeV/c (the incident energy that produces the greatest significance for the 320 μm tracker). The second two are the maximum incident momenta that provide separations of $S = 2$ and $S = 1$, respectively. These four points of comparison are shown in Table 4.1 for each weight ratio that was studied. Table 4.1 also repeats the results of Chapter 3 for the 20 μm and 320 μm homogeneous trackers, for ease of comparison.

weight	T	S_{150}	S_{230}	$2S$(MeV/c)	$1S$(MeV/c)
1:1	3	7.70	6.18	605	850
4:1	2	6.73	5.48	592	829
8:1	3	6.54	5.97	596	814
12:1	3	7.24	6.86	624	846
16:1	4	8.26	7.99	657	874
20:1	5	9.41	8.82	683	904
24:1	7	9.91	9.07	692	918
28:1	7	9.41	8.38	699	935
32:1	8	8.49	8.03	693	935
36:1	8	7.98	7.77	691	936
40:1	8	7.71	7.65	688	935
20 μm	6	8.62	7.21	581	765
320 μm	7	8.14	11.3	842	1020

Table 4.1: Summary table of four points of comparison in the heterogeneous tracker as a function of the weight ratio. The "weight" column shows the factor by which the thin layer energy losses were scaled relative to the those of the thick layers. The contents of Table 3.2 have been included at the bottom, for easier comparison.

Figures 4.1 through 4.6 show the K-π separation as a function of incident momentum for weights of 1:1, 8:1, 16:1, 24:1, 32:1, and 40:1, respectively. For each figure, the significance trajectory for the optimal value of T is displayed, as well as the trajectory for $T = 0$ and for a value of T a few units larger than the optimal trajectory

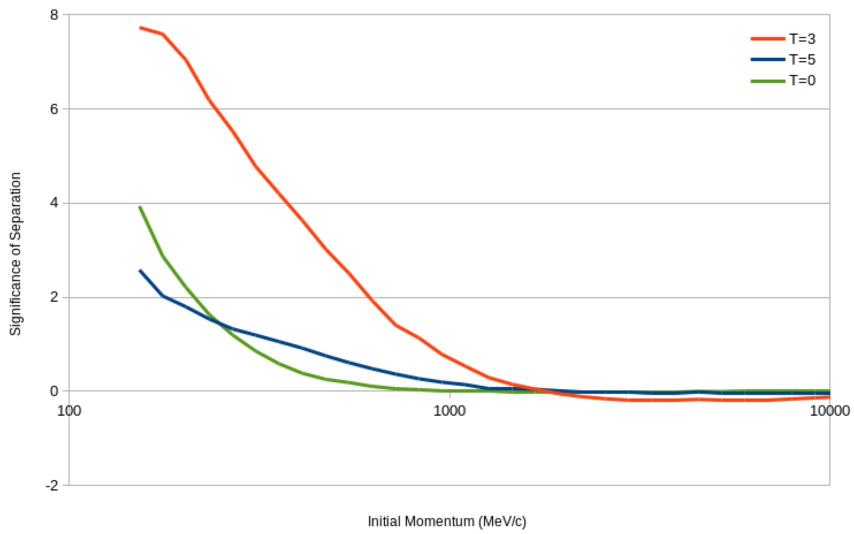

Figure 4.1: Significance trajectories for the heterogeneous tracker with a 1:1 weighting.

in order to get a sense of the degradation that arises from over-truncation.

The performance of the heterogeneous tracker is seen to improve with increased weight ratio, reaching an optimum significance of separation at a weight ratio of approximately 24:1 for lower incident momentum, and 28:1 for incident momentum approaching 1 GeV/c. This is somewhat surprising, in that the ratio of layer thicknesses, and thus of the most likely energy loss, is 16:1, significantly less than the observed optimal ratio of 24:1. In addition, the ratio of the width to the mean of the energy loss is greater for the 20 μm thickness, which would naively suggest that one might expect a weight ratio smaller than the thickness ratio of 16:1 to produce optimal results. Developing an understanding of this behavior would be an interesting avenue for further study.

After optimization, the K-π separation performance of the heterogeneous tracker is seen to lie between that of the two homogeneous trackers, which is expected since the heterogeneous tracker is a mixture of layers from the 20 μm and 320 μm trackers. The exception to this is at the lower energy bound of 150 MeV/c, where the separation power of the heterogeneous tracker seems to exceed that of both the 20 μm and 320 μm homogeneous trackers. This is most likely due to the fact that many of the kaons that get absorbed in the 320 μm homogeneous detector are able to make it all the way through the heterogeneous detector, providing more layers for the measurement of energy loss.

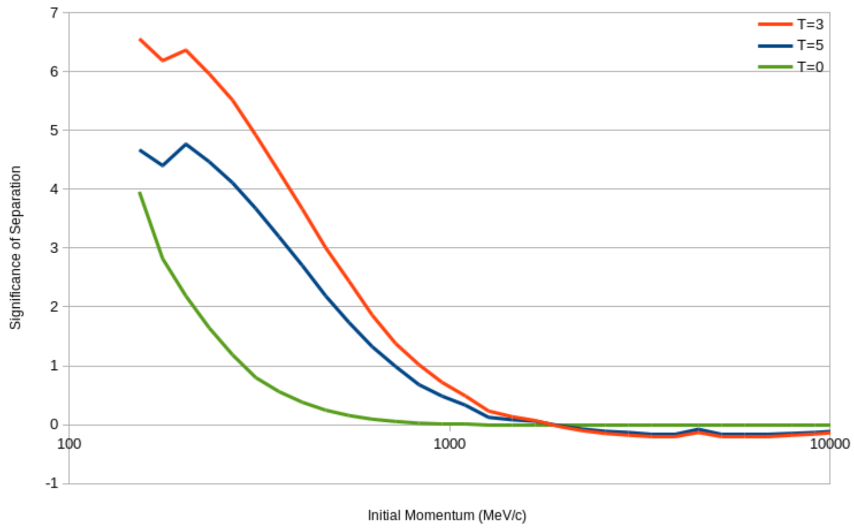

Figure 4.2: Significance trajectories for the heterogeneous tracker with a 8:1 weighting.

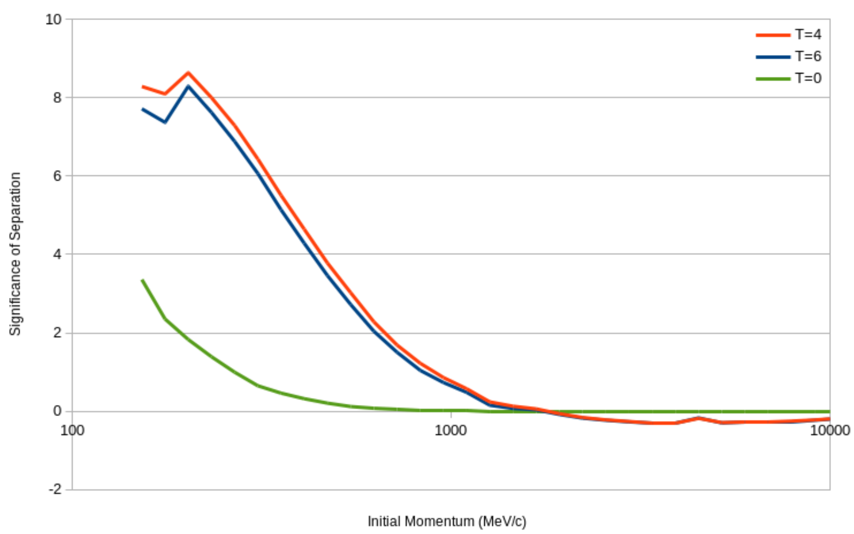

Figure 4.3: Significance trajectories for the heterogeneous tracker with a 16:1 weighting.

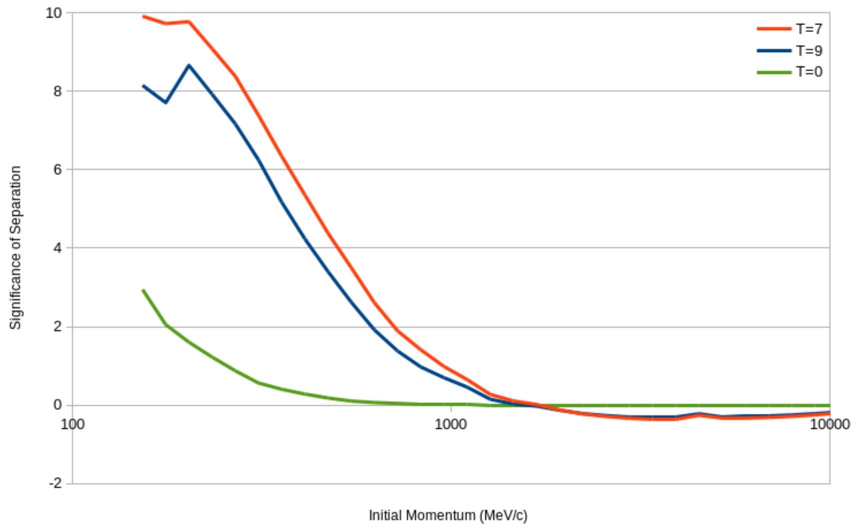

Figure 4.4: Significance trajectories for the heterogeneous tracker with a 24:1 weighting.

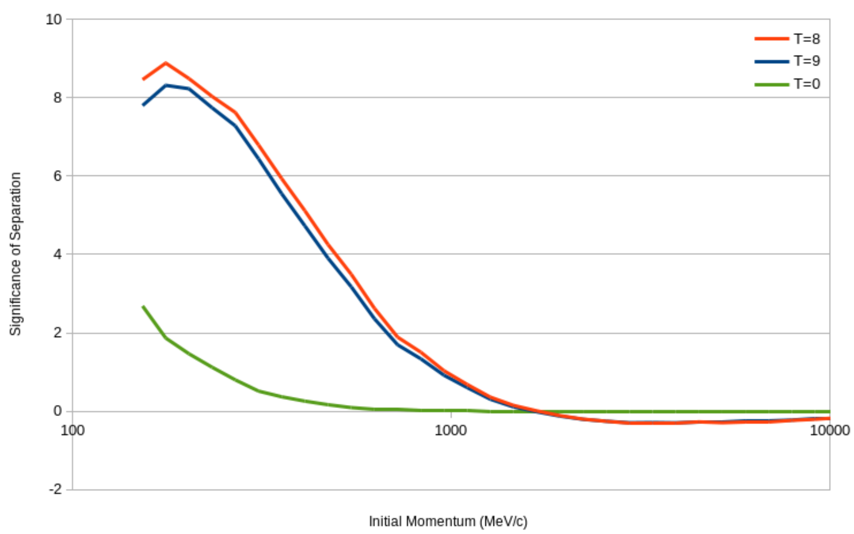

Figure 4.5: Significance trajectories for the heterogeneous tracker with a 32:1 weighting.

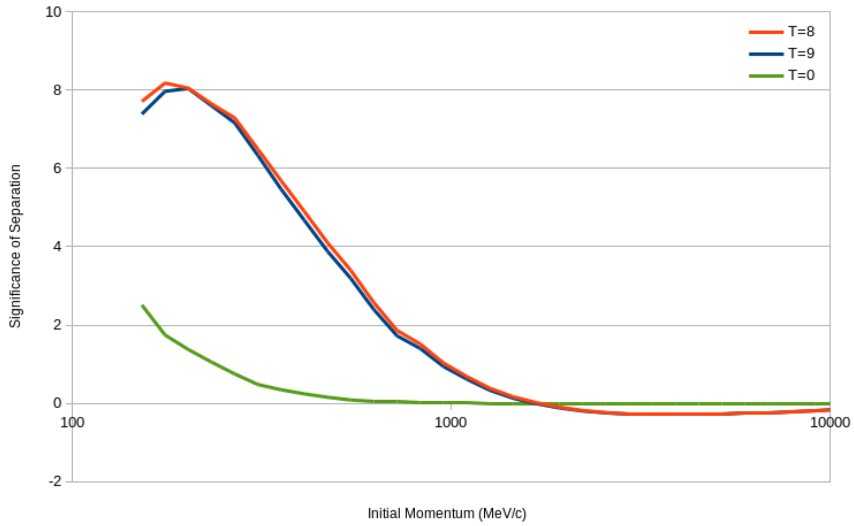

Figure 4.6: Significance trajectories for the heterogeneous tracker with a 40:1 weighting.

It's interesting to note that the low-incident-momentum performance of the heterogeneous tracker begins to degrade as the weight ratio increases beyond 24:1, while for incident momenta about 500 MeV/c or so, the performance remains robust even for the 40:1 weight ratio. This suggests that the use of weight ratios that vary with incident momentum might yield the best K-π separation performance for the heterogeneous tracker. The maximum of the range over which kaons and pions can be distinguished to better than two (one) standard deviations by the heterogeneous tracker is relatively stable with respect to the weight ratio, reaching values of about 690 (940) MeV/c for weight ratios above 28:1.

5 Conclusion

The purpose of these studies was to assess the ability of a colliding beam detector tracking system composed of layers of silicon sensors of varying thickness to perform particle identification via the measurement of mean energy loss. The significance of separation between the kaon and pion energy loss distributions was chosen to be the metric of the particle ID performance. The interest in separating a kaon from a pion via energy loss measurements in solid state trackers arises from heavy flavor production in colliding beam experiments, which has a strong tendency to produce kaons. To achieve this goal, the energy-loss MC simulation program SimSIdE [5] was significantly modified to match expectations for the mean and variance of the energy-loss distributions from Refs. [1, 6].

Three tracker configurations were considered: two homogeneous trackers each composed of 10 layers of either 20 μm or 320 μm silicon, and a heterogeneous tracker composed of 5 layers of 20 μm silicon followed by 5 layers of 320 μm silicon. The two homogeneous trackers were considered as points of comparison for the heterogeneous tracker, which represents the baseline configuration of the tracking system of two of the three detector systems being designed for use at prospective new electron-positron linear colliders.

The precise measurement of energy loss for multi-layered detectors such as these requires the use of truncation to remove the highest loss layers, cropping off the Landau tail of the energy loss distributions to significantly increase the ratio of mean of the energy loss distribution to its variance. Independent of the thickness of the layers and the momentum of the incident particles, optimal performance was achieved for truncation of greater than 50% of the tracking layers, and as much as 80% of the layers, which was somewhat unexpected.

The energy losses in the thin layers of the heterogeneous tracker were multiplied by a weighting factor before truncation so that the information from the thin layers would make a significant contribution to the energy loss mean, and to ensure that losses from the Landau tail would be truncated as readily as those from the thicker layers. A range of weighting factors from 1 to 40 were examined. For lower incident momentum (several hundred MeV/c or less), the optimal weight ratio (i.e., the weight factor achieving the highest possible significance of separation) was found to be around 24:1, while for incident momenta approaching 1 GeV/c the optimal weight was found to be somewhat higher, with a plateau in the performance for a range of weighting factors between 28:1 and 40:1.

As expected, the optimized performance of the heterogeneous tracker lay somewhat between that of the 20 μm and 320 μm homogeneous tracker, since it is composed of equal amounts of each thickness of the two homogeneous trackers. The maximum observed significance of separation for the heterogeneous tracker was found to be $S = 9.91$ for an incident momentum of 150 MeV; this performance was achieved with a weighting factor of 24:1. The maximum range found for a significance of separation of $S = 1$ was 936 MeV/c at a weight of 36:1 while the maximum range for $S = 2$ was 699 MeV/c, for a weight of 28:1. K-π separation using energy loss measurements in silicon for incident momenta approaching and exceeding 1 GeV/c seems very difficult.

Three items requiring further inquiry were identified during the study. For a homogeneous tracker with 20 μm thick layers, a small plateau in the generally decreasing mean energy loss was observed for kaons of an incident momentum of $\sim$175 MeV/c. In addition, the optimal weighting factor for the thinner layers of the heterogeneous tracker is found to be significantly greater than the naive upper bound of 16:1 (the ratio of thicknesses). Finally, the effects of Gaussian electronic noise seem significant in the estimation of the $S = 1, 2$ ranges. The cause of these observations remains unknown, but would be interesting and perhaps revealing to understand.

A | Obtaining and Using SimSIdE and my Simulations

All source code can be found online at:
http://scipp.ucsc.edu/~schumm/dEdX/

These simulations were compiled via the GNU Compiler Collection.
Specifically g++ v4.4.7.

Bibliography

[1] Hans Bichsel. Straggling in thin silicon detectors. *Rev. Mod. Phys.*, 60:663–699, Jul 1988.

[2] David R. Bickel and Rudolf Fruehwirth. On a fast, robust estimator of the mode: Comparisons to other robust estimators with applications. 2005.

[3] CERN. CLHEP- A class library for high energy physics. Available at http://proj-clhep.web.cern.ch/proj-clhep/ (2018/06/08).

[4] L. Landau. On the energy loss of fast particles by ionization. *J. Phys.(USSR)*, 8:201–205, 1944.

[5] G Lynch. SimSIdE. original software, 1993.

[6] C. Patrignani et al. Review of Particle Physics. *Chin. Phys.*, C40(10):100001, 2016.

[7] John R. Sabin. Determination of the mean excitation energy of materials for projectile stopping power. *Journal of Physical Chemistry Biophysics*, 4(1):1–2, 2014.

[8] R.M. Sternheimer, M.J. Berger, and S.M. Seltzer. Density effect for the ionization loss of charged particles in various substances. *Atomic Data and Nuclear Data Tables*, 30(2):261 – 271, 1984.